9-26-2003

Regulation of Na,K-ATPase by PLMS, the Phospholemman-Like Protein From Shark: Molecular Cloning, Expression, Cellular Distribution and Functional Effects of PLMS

Yasser A. Mahmmoud
University of Aarhus

Gordon Cramb
University of St. Andrews

Arvid B. Maunsbach
University of Aarhus

Christopher P. Cutler
Georgia Southern University, ccutler@georgiasouthern.edu

Lara Meischke
University of St. Andrews, theasc@st-andrews.ac.uk

Recommended Citation

Mahmmoud, Yasser A., Gordon Cramb, Arvid B. Maunsbach, Christopher P. Cutler, Lara Meischke, Flemming Cornelius. 2003. "Regulation of Na,K-ATPase by PLMS, the Phospholemman-Like Protein From Shark: Molecular Cloning, Expression, Cellular Distribution and Functional Effects of PLMS." *Journal of Biological Chemistry*, 278 (39): 37427-37428. doi: 10.1074/jbc.M305126200 source: https://www.sciencedirect.com/science/article/pii/S0021925820833031?via%3Dihub
https://digitalcommons.georgiasouthern.edu/biology-facpubs/67

THE JOURNAL OF BIOLOGICAL CHEMISTRY
Vol. 278, No. 39, Issue of September 26, pp. 37427–37438, 2003
Printed in U.S.A.

Regulation of Na,K-ATPase by PLMS, the Phospholemman-like Protein from Shark

MOLECULAR CLONING, SEQUENCE, EXPRESSION, CELLULAR DISTRIBUTION, AND FUNCTIONAL EFFECTS OF PLMS*

Received for publication, May 15, 2003, and in revised form, July 14, 2003
Published, JBC Papers in Press, July 21, 2003, DOI 10.1074/jbc.M305126200

Yasser A. Mahmmoud‡, Gordon Cramb§, Arvid B. Maunsbach¶, Christopher P. Cutler§, Lara Meischke§, and Flemming Cornelius‡‖

From the ‡Department of Biophysics, University of Aarhus, Ole Worms Allé 185, DK-8000 Aarhus C, Denmark, ¶The Water and Salt Research Centre, Department of Cell Biology, Institute of Anatomy, University of Aarhus, DK-8000 Aarhus C, Denmark, and the §School of Biology, Bute Medical Bldgs., University of St-Andrews, Fife KY16 9TS, United Kingdom

In Na,K-ATPase membrane preparations from shark rectal glands, we have previously identified an F*X*YD domain-containing protein, phospholemman-like protein from shark, PLMS. This protein was shown to associate and modulate shark Na,K-ATPase activity *in vitro*. Here we describe the complete coding sequence, expression, and cellular localization of PLMS in the rectal gland of the shark *Squalus acanthias*. The mature protein contained 74 amino acids, including the N-terminal F*X*YD motif and a C-terminal protein kinase multisite phosphorylation motif. The sequence is preceded by a 20 amino acid candidate cleavable signal sequence. Immunogold labeling of the Na,K-ATPase α-subunit and PLMS showed the presence of α and PLMS in the basolateral membranes of the rectal gland cells and suggested their partial colocalization. Furthermore, through controlled proteolysis, the C terminus of PLMS containing the protein kinase phosphorylation domain can be specifically cleaved. Removal of this domain resulted in stimulation of maximal Na,K-ATPase activity, as well as several partial reactions. Both the $E_1{\sim}P \rightarrow E_2$-P reaction, which is partially rate-limiting in shark, and the K^+ deocclusion reaction, $E_2(K) \rightarrow E_1$, are accelerated. The latter may explain the finding that the apparent Na^+ affinity was increased by the specific C-terminal PLMS truncation. Thus, these data are consistent with a model where interaction of the phosphorylation domain of PLMS with the Na,K-ATPase α-subunit is important for the modulation of shark Na,K-ATPase activity.

The Na,K-ATPase is the enzyme responsible for active transport of Na^+ and K^+ across the plasma membranes of animal cells (for recent review, see Ref. 1). It establishes and maintains the electrochemical gradients for Na^+ and K^+ responsible for generation of a resting membrane potential necessary for excitability of muscle and nerve cells, co- and counter-transport of ions and nutrient molecules across the cell membrane, as well as the regulation of cell volume. The enzyme is composed of two essential subunits; a catalytic α-subunit, which undergoes conformational changes that couple ATP hydrolysis to ion transport, and the heavily glycosylated β-subunit responsible for maturation, assembly, and membrane targeting of the enzyme. Different isoforms of the α- and β-subunit have been identified, and these have unique kinetic properties and tissue distributions.

As a housekeeping enzyme the regulation of the Na,K-ATPase is very complex and occurs at many different levels, including both rapid (short term) and sustained (long term) hormonal control. Recently, considerable interest have been directed at studying the role of protein-protein interactions in the acute hormonal regulation of Na,K-ATPase activity. Indeed, regulation of transport ATPases by interaction with small regulatory proteins is a well known mechanism to achieve modulation of ATPase activity *in vivo* (for review see Ref. 2). Such interactions are especially well described for the regulation of SERCA[1] by phospholamban (PLN) and sarcolipin (3–7).

The small protein called the γ-subunit is the first example of a small single transmembrane protein interacting with and regulating Na,K-ATPase (8–10). The γ-subunit has been shown to modulate Na,K-ATPase activity in the kidney by affecting the E_2/E_1 equilibrium toward E_1, thus regulating the affinity for ATP at its low affinity site and the cytoplasmic Na^+ and K^+ competition (11). The γ-subunit has a highly distinct distribution along different parts of the nephron allowing differential regulation of ion transport along different nephron segments (12).

The γ-subunit is a member of a family of small hydrophobic proteins, now termed the F*X*YD domain-containing protein family (13). This family includes phospholemman (PLM or F*X*YD1) (14), the γ-subunit (F*X*YD2) (15), mammary tumor protein of 8-kDa molecular mass (MAT-8 or F*X*YD3) (16), channel-inducing factor (CHIF or F*X*YD4) (17), related to ion channel (RIC or FYXD5) (18), as well as F*X*YD6 and F*X*YD7.

Until recently the physiological functions of the F*X*YD pro-

* This work was supported by the Danish Medical Research Council, Aarhus University Research Foundation, the A. P. Møller foundation, The Novo Nordic Foundation (to F. C. and Y. A. M.), and The Danish Natural Research Foundation (to A. B. M.). The Federation of the European Biochemical Societies (FEBS) is acknowledged for providing an FEBS summer fellowship (to Y. A. M.) to perform the cloning work. The costs of publication of this article were defrayed in part by the payment of page charges. This article must therefore be hereby marked "*advertisement*" in accordance with 18 U.S.C. Section 1734 solely to indicate this fact.

The nucleotide sequence(s) reported in this paper has been submitted to the GenBank™/EBI Data Bank with accession number(s) AJ556170.

‖ To whom correspondence should be addressed. Tel.: 45-8942-2926; Fax: 45-8612-9599; E-mail: fc@biophys.au.dk.

[1] The abbreviations used are: SERCA, sarcoplasmic-endoplasmic reticulum calcium ATPase; PLN, phospholamban; PKA, protein kinase A; PKC, protein kinase C; DTT, dithiothreitol; RACE, rapid amplification of cDNA ends; MOPS, 4-morpholinepropanesulfonic acid; MES, 4-morpholineethanesulfonic acid; PBS, phosphate-buffered saline; Tricine, *N*-[2-hydroxy-1,1-bis(hydroxymethyl)ethyl]glycine; CDTA, 1,2-cyclohexylenedinitrilotetraacetic acid; EST, expressed sequence tag.

teins (except F*X*YD2) were unknown. However, it has now become evident that they are tissue-specific regulators of ion transporters (see recent reviews, Refs. 19 and 20). Originally, this idea was substantiated by the identification of a PLM homologue (phospholemman-like protein from shark, PLMS) that was shown to specifically interact with and modulate Na,K-ATPase in the shark rectal gland (21). Subsequent investigations by Crambert *et al.* (22), who used a co-expression system to study the effects of mammalian F*X*YD1 on Na,K-ATPase activity, indicated that PLM interacts with and regulates Na,K-ATPase isoforms. Indeed, both F*X*YD 4 (CHIF) and F*X*YD7 have been recently reported to be tissue-specific regulators of Na,K-ATPase (23, 24). Therefore, it seems conceivable that most, if not all, members of the F*X*YD protein family are tissue-specific regulators of Na,K-ATPase.

The regulatory interaction of Na,K-ATPase with F*X*YD proteins seems to play an important role in cellular physiology and pathophysiology. For instance, the physiological relevance of the γ-subunit has recently been substantiated by identification of a point mutation of a glycine residue, which is highly conserved among all F*X*YD proteins, which correlates with a renal magnesium deficiency (25). In addition, phenotypic analysis of CHIF knockout mice indicated that CHIF plays a vital role in the tolerance to high K^+ loading (26). Thus, characterization and localization of F*X*YD proteins in different tissues represents an important aim in identifying regulatory mechanisms of ion transport under physiological and pathophysiological states.

Little is known about the three-dimensional functional interactions leading to regulation of the Na,K-ATPase by F*X*YD proteins. Spatial localization of the γ-subunit has been indirectly inferred from cryo-electron microscopy of two-dimensional crystals (27) or from thermal denaturation experiments (28). They seem to indicate that the γ-subunit is associated with the C terminus of the α-subunit being located either between the M2/M9 or the M9/M10 transmembrane segments. Recently, the kinetic effects of γ on Na,K-ATPase were allocated to distinct domains within the γ-subunit (29). Also, mutagenesis studies of both the γ-subunit and CHIF indicated that the F*X*YD motif was important for long term and stable association with the α-subunit, whereas the basic residues located at the C terminus of CHIF are not necessary for association but are important determinants for the functional effects of CHIF on Na,K-ATPase (23). Recently it was demonstrated that residues in the transmembrane segment of γ and CHIF are important for their association with and regulation of the Na,K-ATPase (30).

PLM and its homologue PLMS are the only members of the F*X*YD family known to be phosphorylated by protein kinases. The C terminus of PLMS is heavily phosphorylated by PKC (21), as is the case for PLM (14). Co-immunoprecipitation experiments demonstrated that dephosphorylated PLMS associated more strongly with the α-subunit than PKC-phosphorylated PLMS (21). This suggests that the interaction between PLMS and the shark α-subunit could be controlled by protein kinase-mediated phosphorylation reactions in a similar way to that proposed for the phospholamban (PLN) regulation of the Ca-ATPase in cardiac tissue in response to hormonal stimulation (3–7). Furthermore, PKC phosphorylation of the C-terminal cytoplasmic domain of PLMS, or disruption of interactions within the transmembrane domain by treatment with non-solubilizing concentrations of the non-ionic detergent $C_{12}E_8$ have been shown to result in activation of the shark Na,K-ATPase by relieving the inhibitory effect of PLMS (21). This again emphasizes the implication of multiple domain interaction between F*X*YD regulatory proteins and Na,K-ATPase, as is the case for PLN regulation of Ca-ATPase.

In the present study we aim to further characterize the molecular interactions that result in the regulation of shark Na,K-ATPase by PLMS. To begin this, we have first cloned PLMS and determined its primary amino acid sequence from cDNA. In addition, we have characterized the cellular distribution of both PLMS and the α-subunit in rectal gland cells using immunocytochemical methods. Finally, through controlled proteolysis we have been able to preferentially cleave a 5-kDa fragment from the C terminus of PLMS, which contains the protein kinase phosphorylation sites. Using this approach, we have characterized the functional effects of the interaction between the C-terminal domain of PLMS and shark Na,K-ATPase. Some results of this study have been previously reported (31).

EXPERIMENTAL PROCEDURES

Total RNA Extraction—Total RNA was extracted using a modification of the Chomczynski and Sacchi method (32) as described previously (33). In brief, tissues were collected and rapidly frozen in liquid nitrogen before transfer and storage at −80 °C. The tissue was pulverized using a mortar and pestle and then homogenized in 10 volumes (w/v) of 4 M guanidinium isothiocyanate, 25 mM sodium citrate, 0.5% (v/v) Sarkosyl, and 90 mM 2-mercaptoethanol using a Polytron PT 10 homogenizer (Kinematica Ltd.) set at position 5, for 2 × 20–30 s. Following homogenization, total RNA was extracted by the sequential addition of 0.1 volume of 2 M sodium acetate, pH 4.0, 0.5 volume of water-saturated phenol, and finally 0.2 volume of 1-bromo-3-chloropropane. Tubes were vortexed briefly between the additions of each solution and then centrifuged at 3900 × *g* for 30 min at 4 °C in a Beckman J6-MC centrifuge (Beckman Instruments Inc.). The upper aqueous phase was carefully transferred to a fresh tube, and then 2.5 volumes of 2-propanol and 0.2 volume of 1.2 M NaCl, 0.8 M sodium citrate, pH 7.0, was added sequentially with vortexing. The resulting solution was incubated at room temperature for 10 min, before centrifugation at 3900 × *g* for 30 min. The supernatant was aspirated, and the pellet was washed twice in 80% ethanol before drying under vacuum at room temperature for 5 min. After resuspension of the pellet in diethylpyrocarbonate-treated Milli-Q water, diluted samples (1:100) were prepared and the absorbance measured at 260 and 280 nm (Philips PU 8620 spectrophotometer) to estimate both the concentration and purity of the RNA samples. RNA samples from each extract were also run on denaturing formaldehyde gels and stained with ethidium bromide (as detailed below) to ensure that no degradation of the RNA had occurred.

Cloning and Sequencing—First strand cDNA synthesis was carried out in a total reaction volume of 20 μl containing 5 μg of total rectal gland RNA, 75 mM Tris-HCl, pH 8.3, 3 mM $MgCl_2$, 10 mM DTT, 10 μM oligo$(dT)_{12–18}$, 1 mM each of deoxyribonucleotide triphosphates (dNTPs; dATP, dGTP, dCTP, and dTTP), and 200 units of Superscript II (Invitrogen, Paisley, UK). The reaction was incubated at 45 °C for 2 h and then stored frozen at −20 °C for use in PCR. This single strand cDNA template was used for the amplification and isolation of the initial 203-bp fragment with the sequences further 5′ or 3′ to this subsequently obtained by rapid amplification of cDNA ends using the Marathon RACE kit (Clontech, Basingstoke, UK) as described previously (33). All PCR reactions were carried out using 0.5 μl of cDNA template in a total volume of 20 μl, comprising 10 mM Tris-HCl, pH 9.0, 50 mM KCl, 1.5 mM $MgCl_2$, 0.2 mM dNTPs, 4 pmol each of sense and antisense primers, and 1.25 unit of *Taq* DNA polymerase (BioGene Ltd., Cambs, UK). Primers used were as follows. Initial amplifications were carried out using Squ-1 sense (CG*X*TTCACTTACGACTACTAC) and Squ-1 antisense (CCGCCTGCGGGTGGACAGACGGCG) primer pairs (*X* = any base). Subsequent nested 5′ and 3′-RACE reactions employed 5′-RACE-1 (CACACAGCACTGCGGCCAC), 5′-RACE-2 (CCACAATCAGTCCGACAACACGC), 3′-RACE-1 (GCGTGTTGTCGGACTGATTGTGG), and 3′-RACE-2 (GTGGCCGCAGTGCTGTGTG) primers in amplifications with the Marathon kit primers AP-1 (CCATCCTAATACGACTCACTATAGGGC) and AP-2 (ACTCACTATAGGGCTCGAGCGGC). PCR was performed using a hot start technique with an initial 2-min incubation at 92 °C, followed by 40 cycles of 94 °C for 5 s, 55 °C for 30 s, and 72 °C for 30 s, with a final incubation of 72 °C for 10 min.

DNA fragments within PCR reactions were either purified directly using an Edge Biosystems Quick-Step PCR purification kit (VH Bio Ltd., Gosforth, UK) or separated by Tris acetate-EDTA-agarose gel electrophoresis (34) and bands of interest were purified using a Geneclean II DNA purification kit (Anachem Ltd., Luton, UK).

3′- and 5′-RACE products were produced in nested PCR reactions using *Squalus* PLMS-specific sense and antisense primers in conjunction with the Marathon kit nested primers AP1 and AP2. PCR fragments generated using the initial primers or by RACE amplification were blunt-ended by incubation for 15 min at 72 °C with 0.025 unit/μl *Pfu* DNA polymerase in 1× *Pfu* buffer (Stratagene) containing 0.2 mM dNTPs and then cloned into TOP10 cells using a Zero Blunt TOPO PCR cloning kit (Invitrogen, Leek, The Netherlands). Positive colonies were identified by colony PCR, and cDNA fragments from at least four different clones were sequenced in both directions using a Big Dye Terminator sequencing kit (PerkinElmer Life Sciences Biosystems, Warrington, UK) as described previously (33). Sequences were combined and analyzed using the GeneJockey II software package (Biosoft, Cambridge, UK).

Northern Blotting—Northern blotting was performed as described previously (33). The probe used for Northern analysis was a full-length cDNA containing the complete sequence shown in Fig. 1. Total RNA (5 μg, as measured by absorbance at 260 nm) extracted from various *Squalus* tissues was resuspended in MOPS buffer (20 mM MOPS, 8 mM sodium acetate, 1 mM EDTA, pH 7.8) containing 12.5 M formamide and 2.2 M formaldehyde and then denatured at 65 °C for 15 min and snap-cooled on ice before adding 0.1 volume of 5% "Loading Dyes" (0.025% bromphenol blue, 0.025% xylene cyanol, and 50% glycerol; all w/v). Samples (30–100 μl) were then loaded onto the agarose gel (1.2% agarose w/v (Biogene Ltd.), MOPS buffer containing 6.7% (v/v) formaldehyde) and electrophoresed at 135 V (5 V/cm) for 1.5–2 h in MOPS buffer. After electrophoresis, gels were stained for 30 min in 0.1 M ammonium acetate, 5 μg/ml ethidium bromide before destaining for 1–2 h in several changes of 0.1 M ammonium acetate before viewing on a UV transilluminator. The integrity and relative amounts of RNA loaded onto each lane were qualitatively assessed by viewing the sharpness and intensity levels of ethidium bromide-stained 18 S and 28 S ribosomal RNA bands as quantified using a gel documentation and analysis system (Syngene, Cambridge, UK). The staining intensities of the tissue rRNA bands were compared with a known standard, and the amount of total RNA loaded on each lane was re-determined. The separated RNAs were electroblotted overnight using TAE (40 mM Tris base, 0.35% (v/v) glacial acetic acid, 10 mM EDTA, pH 8.0) as blotting buffer (25 V, 0.75 amps) onto a Zeta Probe nylon membrane (Bio-Rad, Hemel Hempstead, UK). RNA blots were prehybridized in 10 ml of UltraHyb (Ambion, Huntingdon, UK) for 6 h at 47 °C and then hybridized overnight in the same solution with the ^{32}P-labeled *Squalus* PLMS probe (Megaprime DNA labeling system, Amersham Biosciences, Little Chalfont, UK). Membranes were washed sequentially at 47 °C in 0.5× SSC, 1% SDS, then 0.2× SSC, 0.1% SDS and finally 0.1× SSC, 0.1% SDS for 15 min before analysis of radioactive intensity by electronic autoradiography (Instant Imager, Canberra Packard Instruments, Meriden, CT). The blots were finally incubated at −80 °C with x-ray film (Kodak BioMax MS) for autoradiography (1× SSC = 0.15 M NaCl, 15 mM sodium citrate, pH 7.0).

Cellular Localization of PLMS and Na,K-ATPase α-Subunit—Salt glands from two sharks were immersion-fixed for 2 h with a solution containing 4% paraformaldehyde, 150 mM NaCl, and 100 mM sodium cacodylate buffer (pH 7.2). Small tissue blocks from the middle of the glands were cryo-protected with 2.3 M sucrose and frozen in liquid nitrogen. Immunoelectron microscopy was performed on thin (60–80 nm) cryosections, which were cut at −120 °C from the frozen tissue on a Reichert Ultracut S cryo-ultramicrotome (Leica, Vienna, Austria).

Immunolabeling and staining was performed as previously described (35). Briefly, the sections were first preincubated in PBS containing 0.1% skimmed milk powder and 50 mM glycine. The sections were then incubated for 1 h at room temperature with rabbit anti-PLMS antibodies, rabbit anti-Na,K-ATPase α-subunit antibodies, or pre-immune sera diluted 1:100–1:1600 in PBS containing 0.1% skimmed milk powder. The primary antibodies were visualized using goat anti-rabbit IgG conjugated to 10-nm colloidal gold particles (GAR.EM1O, Bio-Cell Research Laboratories, Cardiff, UK) diluted 1:50 in PBS with 0.1% skimmed milk powder and polyethylene glycol (5 mg/ml). The Ultrathin cryosections were stained with uranyl acetate in methylcellulose before examination in a Zeiss 912 or a Philips 208 electron microscope. Immunolabeling controls consisted of substitution of the primary antibody with rabbit pre-immune IgG or incubation without primary antibody. All controls showed absence of specific labeling.

Na,K-ATPase Preparation and Hydrolytic Activity—In this study, purified Na,K-ATPase-containing membranes from the rectal gland of *Squalus acanthias* were used. Purification of membrane fragments was as previously described (36). Protein concentrations, ranging from 3 to 5 mg/ml, were determined using Peterson's modification of the Lowry method (37), using bovine serum albumin as a standard. The specific activity was ~ 30 units/mg at 37 °C and 10.5 units/mg at 24 °C (1 unit = 1 μmol of P_i/min). The ATPase activity was measured in a reaction mixture containing 30 mM histidine, pH 7.4, 3 mM $MgCl_2$, 0.06% bovine serum albumin, 10% glycerol, 10 μM ATP (containing 0.03 μCi of γ-[^{32}P]ATP), and variable concentrations of NaCl, KCl, and ATP as indicated in separate figure legends. The concentration of P_i hydrolyzed from ATP was measured as previously described (38).

PKA and PKC Phosphorylation of Na,K-ATPase—PKA phosphorylation was performed in a reaction mixture containing 50 mM Hepes, 10 mM $MgCl_2$, 1 mM EGTA, 0.1 mM ATP (Tris salt) containing γ-[^{32}P]ATP (3 μCi/pmol), 0.1% Triton X-100, 4 μg of protein, and 2 milliunits of PKA. The catalytic subunit of PKA was purchased from Sigma. PKC phosphorylation was performed in a typical assay mixture containing 50 mM Hepes, 10 mM $MgCl_2$, 0.5 mM $CaCl_2$, 20 μM L-α-phosphatidylserine (Avanti Polar Lipids, Alabaster, AL), 10 μM dioleoyl 1, 2-*sn*-glycerol (Sigma, St. Louis, MO), 100 μM ATP (Tris-salt) containing 3 μCi/pmol γ-[^{32}P]ATP, 4 μg of protein, and 0.13 μg of purified PKC. PKC was from Calbiochem (La Jolla, CA), and contained the Ca^{2+}-dependent (conventional) isoforms (α, β_I, β_{II}, and γ). The phosphorylation reaction for both kinases was initiated by the addition of ATP, allowed to proceed for 30 min at 24 °C, and terminated by the addition of 16 μl of electrophoresis sample buffer (39).

Gel Electrophoresis and Immunoblotting—The phosphorylated proteins were separated using Tricine-based SDS-PAGE (3% resolution gel, 9% intermediate, and 16% resolving gels, unless indicated elsewhere). Molecular weight standards were from Bio-Rad (Hercules, CA). For the detection of ^{32}P-assisted kinase phosphorylation, the gels were stained with Coomassie Blue, destained, dried, and then analyzed by autoradiography overnight at −80 °C. For immunoblotting, proteins were transferred to polyvinylidene difluoride membranes, then washed for 1 h with PBS buffer containing 5% Tween 20, and incubated overnight at room temperature with primary antibody. The membranes were washed again with PBS and incubated with goat anti-rabbit antibody for 2 h. After washing, the proteins were detected using ECL reagents (Amersham Biosciences). For the detection of the α-subunit from shark rectal gland and pig kidney, the antibody NKA1002–1016 was used (kindly provided by Jesper V. Møller, Department of Biophysics, University of Aarhus).

Preparation of Trypsinized PLMS—To obtain cleavage of the C terminus of PLMS, membrane-bound enzyme was incubated with trypsin (w/w trypsin to protein 1:1000) for 0–10 min on ice in the presence of 130 mM NaCl or 20 mM KCl, plus 1 mM EDTA. The trypsinization reaction was started by the addition of trypsin and stopped by adding a 10-fold excess of soybean trypsin inhibitor. The mixtures was diluted 10-fold with imidazole buffer (25 mM) and centrifuged at 170,000 × *g* for 1 h. The membranes were washed with imidazole and centrifuged again, then finally suspended in a 30 mM histidine buffer, pH 7.4, containing 25% glycerol, and stored at −20 °C. All procedures were carefully performed on ice.

Production of an Antibody to PLMS—Anti-PLMS antiserum was prepared by injection of rabbits with PLMS resolved by SDS-PAGE together with Freund's adjuvant as previously described (40). Characterization and epitope mapping of this antibody will be described elsewhere.

RH421 Fluorescence Measurements—Time-resolved RH421 fluorescence was measured using a rapid mixing stopped-flow spectrofluorometer (SX.17MV, Applied Photophysics) as previously described (41). At all conditions the flow volume was 100–300 μl. The excitation wavelength was 546 nm (using a combined xenon/mercury lamp), and fluorescence was measured at emissions ≥ 630 nm using a cut-off filter. The dead time for the stopped-flow apparatus was about 1.5 ms.

To measure RH421 fluorescence associated with ATP phosphorylation of Na,K-ATPase, one syringe contained 1.6 ml of 25 mM histidine buffer (containing 20 μg of protein) and 0.4 μg of RH421. The second syringe contained 2.0 ml of 10 mM HEPES/MES buffer, or 30 mM imidazole, adjusted with *N*-methyl-D-glucamine to pH 7.5 in the presence various amounts of Na, K, Mg^{2+}, or ATP as specified in separate figure legends.

The E_2 to E_1 reaction was measured essentially as described by Humphrey *et al.* (42) at conditions where one syringe contained 25 mM histidine buffer (containing 20 μg of protein), 0.5 mM CDTA to quench the Mg^{2+}, and 0.4 μg of RH421. The second syringe contained 100 mM NaCl, 2 mM ATP, and 0.5 mM CDTA.

K^+-supported dephosphorylation was measured by mixing Na,K-ATPase pre-phosphorylated by ATP (1 mM) in the presence of Na^+ (100 mM) and Mg^{2+} (4 mM) in HEPES/MES buffer in one syringe, with 20 mM K^+ in the same buffer in the second syringe.

FIG. 1. ***Squalus* PLMS interleaved nucleotide and amino acid sequence.** The *double lines* indicate the putative leader sequence, and the putative transmembrane domain is indicated by the *single solid line*. Potential phosphorylation sites for PKA and PKC are indicated in *boldface* and *framed*. Possible trypsin cleavage sites are indicated by ↓.

RESULTS

Cloning and Sequencing of PLMS—The initial *Squalus* PLMS cDNA fragment to be cloned was amplified using oligonucleotide primers based on the known PLMS amino acid sequence around the F*X*YD motif (21) and a C-terminal consensus sequence based on information from all known mammalian phospholemman proteins (43). Initial amplifications using a specific sense primer (Squ-1 sense) to the known RFTYDYY motif within the previously isolated peptide and a specific antisense primer (Squ-1 antisense) based on the RRLSTRRR motif found at the C terminus of the known mammalian proteins resulted in the amplification of a 203-bp fragment. When analyzed, this fragment encoded the expected amino acid sequence of the isolated peptide (with the exception of leucine replacing lysines at positions 19 and 24) plus 18 other amino acids before a premature stop codon was encountered. Because the 3′-end of the amplicon exhibited no homology to any known F*X*YD gene, specific sense (3′-RACE, 1; 3′-RACE, 2) and antisense (5′-RACE, 1; 5′-RACE, 2) primers were synthesized 5′ to this region where there was still nucleotide and amino acid homology to other F*X*YD proteins. Nested RACE reactions incorporating PLMS-specific primers in combination with AP1 and AP2 primers were then used along with the Marathon cDNA template to amplify 5′- and 3′-ends of the cDNA. When the 3′-RACE products were cloned and sequenced, it was clear that the amplification of the original 203-bp fragment was due to mispriming of the antisense primer with the last 107 nucleotides having no homology with any F*X*YD genes. The final nucleotide sequence based on the consensus sequence of all cloned fragments is shown in Fig. 1. Following the results of the initial Northern analyses (see below) repeated attempts using the 3′-RACE procedure failed to amplify any fragment larger than 318 bp. Although a short poly(A) sequence was present at the 3′-end, there was no obvious signs of a polyadenylation signal in the short 3′-untranslated region.

The cDNA sequencing showed that the protein consisted of 94 amino acids (Fig. 1) and contained a putative 20-amino acid N-terminal signal sequence (44), giving a mature protein with a length of 74 amino acids. The hydropathy plot (not shown) indicates the precursor protein has a hydrophobic amino terminus with one putative transmembrane domain approximately extending between amino acids 40 and 60. The hydrophobic transmembrane domain contains a leucine-isoleucine zipper motif conserved in many F*X*YD proteins and probably responsible for the strong tendency of some F*X*YDs to form oligomeric structures (2). The protein is thus a typical type I protein that is initially targeted to the endoplasmic reticulum by a cleavable N-terminal signal sequence and subsequently anchored in the plasma membrane by a stop-transfer sequence. The cytoplasmic domain contains several basic residues, two conventional protein kinase phosphorylation sites (Thr-53 and Ser-55), and several additional putative phosphorylation sites. There are six potential trypsin cleavage sites at the C-terminal end (positions 42, 44, 46, 51, 52, and 54) just in front and partially overlapping the conventional phosphorylation sites.

Comparison with Mammalian and Teleost FXYD Proteins—Fig. 2 compares the PLMS sequence with the sequences of the known seven F*X*YD proteins found in humans as an example of mammalian species. In addition to the mammalian species, three gene products from the zebrafish, *Danio rerio*, are homologues of the F*X*YD proteins (F*X*YD6dr, F*X*YD8dr, and F*X*YD9dr in the provisional terminology suggested by Sweadner and Rael; Ref. 13). Although there is high conservation of the amino acid sequence in the transmembrane signature motif, there are certain differences between the shark and teleost transcripts and most other mammalian F*X*YD containing proteins. The F*X*YD amino acid motif, which is common to all mammalian members of this family, is altered to F*X*FD in F*X*YD9dr and one of the phospholemman-like proteins cloned from the Japanese Medaka, F*X*YD.b (Fig. 2). However, as

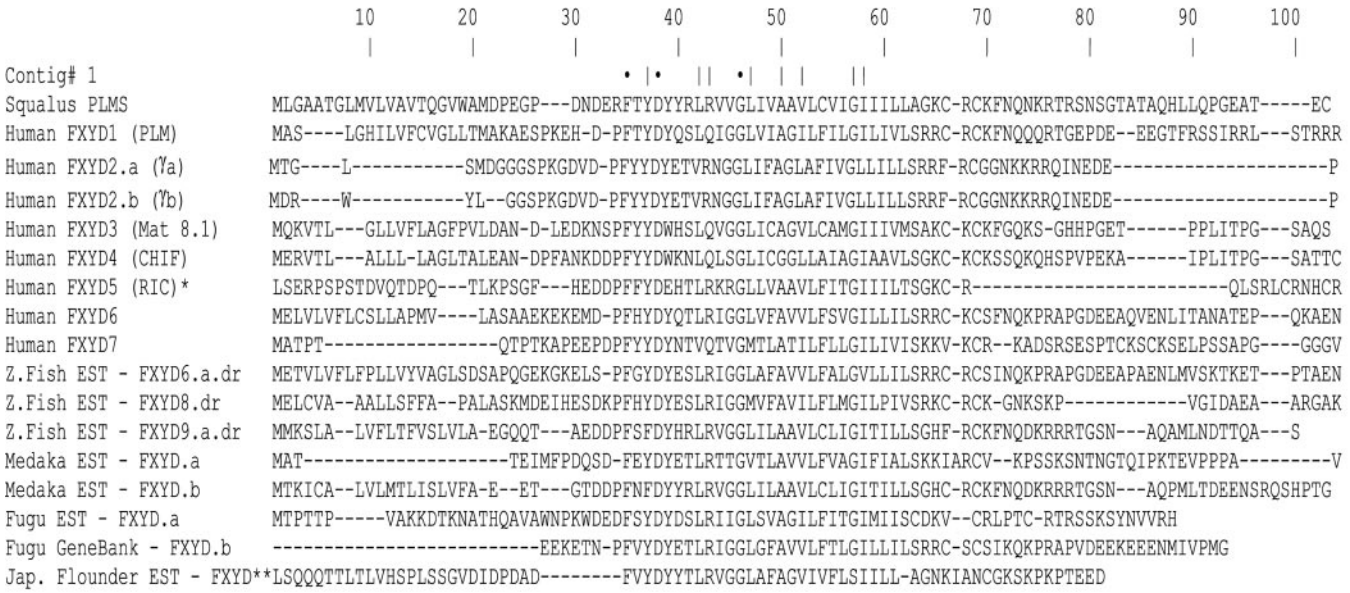

FIG. 2. **The amino acid sequence of *Squalus* PLMS aligned with known human F*XYD* family members and published sequences from teleost fish.** The amino acid sequence of *Squalus* PLMS aligned with known human F*XYD* family members and related EST sequences from various teleost fish. It should be noted that the sequences based on the teleost ESTs should be considered to be provisional, because they are based on single unverified sequence runs. Variant sequences have been reported for the human gamma (F*XYD*2) and for a number of teleost ESTs and in these cases selected sequences (designated with "*.a*" and/or "*.b*") have been reproduced here for comparison with *Squalus* PLMS. *Dots* (·) indicate positions of amino acid identity, and *lines* (|) indicate positions of amino acid similarity. Accession numbers are, *Squalus* PLMS, AJ556170; h*FXYD*1, NM005031; h*FXYD*2.a, NM001680; h*FXYD*2.b, NM021603; h*FXYD*3, NM005971; h*FXYD*4, NM173160; h*FXYD*5, NM014164; h*FXYD*6, NM022003; h*FXYD*7, NM022006; zebrafish F*XYD*6.a.dr, AW153757; zebrafish F*XYD*8dr, AI958251; zebrafish F*XYD*9.a.dr, AW455046; Medaka F*XYD*.a, AU169681; Medaka F*XYD*.b, AU169966; Fugu F*XYD*.a, CA332188; Fugu F*XYD*.b, Fugu genome Gene Bank, FRUP155492/scaffold 2793; Japanese flounder F*XYD*, AU090441. The *asterisks* (* and **) show N-terminal truncated versions of the published sequences. The N-terminal extension for *, the h*FXYD*5, is SPSGRLCLLTIVGLILPTRGQTLKDTTSSSSADSTIMDIQVPTRAPDAVYTELQPTSPTPTWPADETPQPQTQTQ-QLEGTDGPLVTDPETHKSTKAAHPTDDTTT; the N-terminal extension for **, the Japanese flounder F*XYD*, is HERHGHTHRHLDRSFSSSV-SSPEHIQTDEATCRLLKHSPH.

found in PLMS, other putative homologues of phospholemman retain the F*XYD* motif in Medaka (F*XYD*.a), Fugu (F*XYD*.a and .b), and the Japanese flounder. The normally conserved proline residue found immediately before the F*XYD* motif in all mammalian proteins is replaced either by a positively charged arginine (*Squalus* PLMS) or a negatively charged aspartic acid residue (Medaka F*XYD*.a, Fugu F*XYD*.a, and Japanese flounder F*XYD*). In addition, the invariant serine, which is ubiquitously found within the signature sequence and is considered to signal the end of the transmembrane domain (Sweadner and Rael (13)), is replaced by either an alanine in both PLMS and Japanese flounder F*XYD* or a cysteine in Fugu F*XYD*.a (Fig. 2). The two invariant glycines at positions 46 and 57 in the consensus sequence in Fig. 2 are retained in all F*XYD* homologues with the exception of Japanese flounder F*XYD* where the second invariant glycine is replaced by a serine. Because ESTs are the result of single sequencing runs, they often contain errors, and thus the sequences for all of the teleost fish in Fig. 2 are tentative.

The derived amino acid sequence of PLMS shares closest homology with Mat-8/F*XYD*3 with 39–45% amino acid identity and 59–67% amino acid similarity to the known mammalian isoforms. The sequence also exhibits high homology (45% identity and 69% similarity) to the zebrafish protein designated F*XYD*9dr (Sweadner and Rael (13)) and to the Medaka F*XYD*.b sequence (48% identity and 66% similarity). Homologies (measured as percent identity/percent similarity) are then reduced when the putative amino acid sequence is compared with mammalian F*XYD*l (32–39/60–65%), F*XYD*4 (31/65%), F*XYD*5 (32–33/53–54%), F*XYD*6 (29–32/57%), F*XYD*2 (19–29/41–47%), and F*XYD*7 (17–18/48%). Likewise, low homologies were also found when comparison were made to the EST sequences for Medaka F*XYD*.a (29/54%), Fugu F*XYD*.a (28/49%), and F*XYD*.b (20/38%) and the Japanese flounder F*XYD* (26/47%) proteins (Fig. 2).

Tissue and Cellular Distribution of PLMS—The distribution of PLMS over a limited number of *Squalus* tissues was examined by Northern blot analyses (Fig. 3). Blots revealed a major transcript of around 3.8 kb with minor transcripts of ~0.8, 1.1, 1.3, and 2 kb also being identified in some tissues. Image analysis of ethidium bromide-stained 28 S and 18 S rRNA bands revealed that the amount of RNA loaded for each tissue varied from 2.3 μg for the eye to 7.7 μg for the brain (Fig. 3). Taking into consideration the amount of total RNA loaded for each tissue, the highest levels of PLMS mRNA expression were found in the rectal gland > intestine > kidney = brain = heart (approximate ratios 10:2:1, respectively). It should be noted, however, that these values are only semi-quantitative at best and represent mRNA levels across selected tissues taken from only one fish. Using Northern blot analyses we were unable to detect any sign of PLMS mRNA expression in the gill, ovary, skin, or eye even after prolonged autoradiographic exposures.

Immunolocalization of PLMS and Na,K-ATPase α-Subunit—The rectal gland is composed of winding tubules formed by tall columnar cells arranged around a central duct or lumen as previously described (45–47). The luminal cell surface exhibits only a few small microvilli (Fig. 4*A*), but the basolateral cell surface is greatly amplified through slender lateral and basal cytoplasmic folds (Fig. 4*B*). Notably, almost the entire base of the cells consists of such thin cytoplasmic folds, which are devoid of mitochondria and abut the basal lamina (Fig. 4*C*), thus comparable to parts of the peritubular surface of amphibian kidney tubules (48).

Immunolocalization of PLMS showed distinct labeling of the entire basolateral cell membrane (Figs. 5*A* and 6*A*), except the most apical part at the tight junction and around the apical

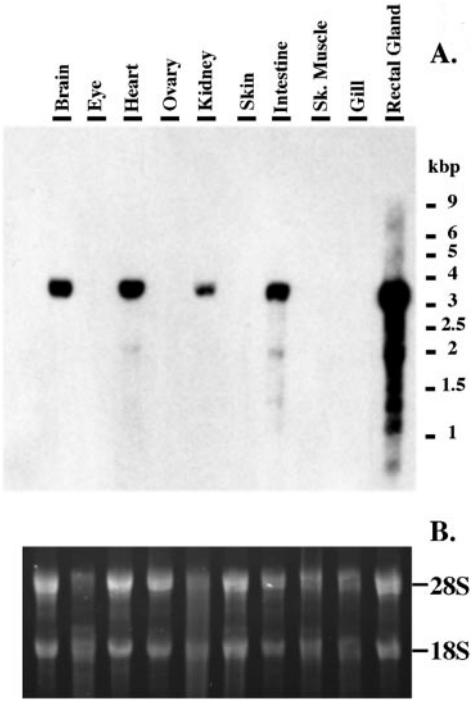

FIG. 3. **Northern blot indicating the expression of PLMS mRNA in selected tissues from *S. acanthias*.** *A*, Northern blot indicating the expression of PLMS mRNA in selected tissues from *S. acanthias*. Total RNA was extracted from each tissue and samples separated by denaturing agarose gel electrophoresis. The gel was stained with ethidium bromide to verify the quantity and assess viability of RNA loaded in each lane (*B*). The amount of total RNA loaded onto each lane was estimated as follows, brain, 7.7 μg; eye, 2.3 μg; heart, 7.6 μg; ovary, 6.0 μg; kidney, 3.8 μg; skin, 6.9 μg; intestine, 4.6 μg; skeletal muscle, 3.5 μg; gill, 3.2 μg; and rectal gland, 6.8 μg. Electroblotting and hybridization with a ^{32}P-labeled PLMS cDNA probe was as detailed under "Experimental Procedures." A major 3.4-kb transcript was identified in the brain, heart, kidney, intestine and rectal gland. Smaller transcripts of ~0.8, 1.1, 1.3, and 2 kb were also detected at much lower abundance in these tissues but were more apparent in the rectal gland, which exhibited the highest levels of expression.

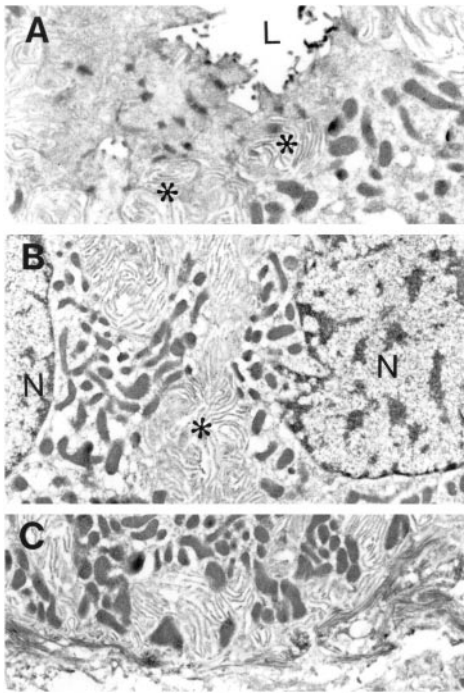

FIG. 4. **Apical (*A*), middle (*B*), and basal (*C*) regions of shark gland cells.** *A*, the apical cell membrane facing the gland lumen (*L*) shows a few short microvilli, but the lateral cell surface exhibits numerous folds projecting into the lateral intercellular space (*). *B*, the lateral intercellular space (*) at the level of the nuclei (*N*) contains extensively interdigitating folds of adjacent cells. *C*, also the basal cell surface is very much amplified through basal folds of the cell membrane. Magnification, ×7000.

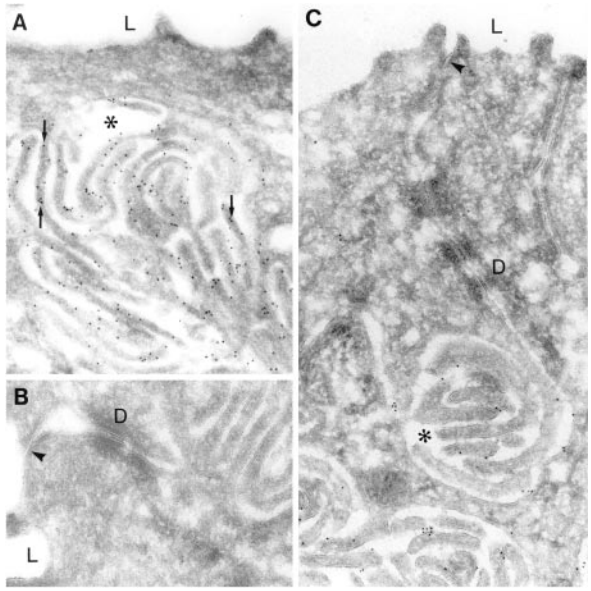

FIG. 5. **Apical parts of shark gland cells.** *A*, immunoelectron microscopy shows extensive PLMS labeling of the lateral cell membrane. Most gold particles are associated with the inner surface of the cell membrane (*arrows*). However, the cell membrane facing the duct lumen (*L*) is unlabeled. *B*, labeling with pre-immune serum is negative. *C*, the localization of Na,K-ATPase is similar to PLMS with labeling of the lateral cell membrane but not the luminal cell membrane. Between the tight junction (*arrowhead*) and the apical desmosomes (*D*) labeling of the cell membrane is usually absent or sparse. Magnification, ×50,000.

desmosomes, where labeling was sparse. Importantly, no labeling was associated with the luminal cell membrane (Fig. 5*A*). The cell membrane of the extensively interdigitating lateral folds was strongly labeled (Figs. 5*A* and 6*A*). Most colloidal gold particles were associated with the cytoplasmic face of the cell membrane, which is consistent with an intracellular localization of the epitope. No label was associated with mitochondria or accumulated in any other part of the cytoplasm. Labeling with pre-immune serum was negative (Fig. 5*B*).

The localization of the Na,K-ATPase α-subunit was similar to that of PLMS. Notably, the luminal cell membrane was unlabeled (Fig. 5*C*) and again much of the label was associated with the cytoplasmic face of the cell membrane (Figs. 5*C* and 6*B*).

Cleavage of the C Terminus of PLMS by Trypsin—As seen in Fig. 1 the sequence of PLMS contains several potential tryptic cleavage sites in the C-terminal cytoplasmic domain upstream of the phosphorylation motif. We have previously described how PKC phosphorylation of PLMS leads to Na,K-ATPase activation caused by impairing of the protein-protein interaction (21). To investigate the nature of such interaction between the PLMS C terminus and the Na,K-ATPase in further details we have undertaken studies to preferentially cleave the PLMS C terminus while keeping the α-subunit intact. This was achieved by using an extremely low concentration of trypsin and incubation for short periods on ice in the presence of the Na,K-ATPase physiological ligands.

Fig. 7 shows the tryptic cleavage pattern of PLMS in the presence of either 130 mM Na^+ or 20 mM K^+. A proteolytic site separating a 5-kDa peptide of PLMS from the intact protein was split by trypsin. In the absence of trypsin, PLMS migrates

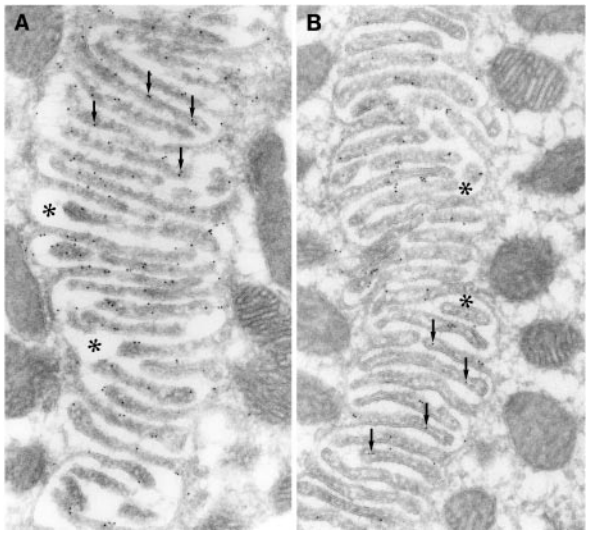

FIG. 6. **Lateral folds of adjacent shark gland cells interdigitate in the lateral intercellular space (*).** The plasma membranes are immunogold labeled for PLMS (*A*) and Na,K-ATPase (*B*), thus demonstrating co-localization of PLMS and Na,K-ATPase. Most immunogold particles are located on the cytoplasmic side of the cell membrane (*arrows*). There is no label over cell organelles or cytosol. Magnification, ×50,000.

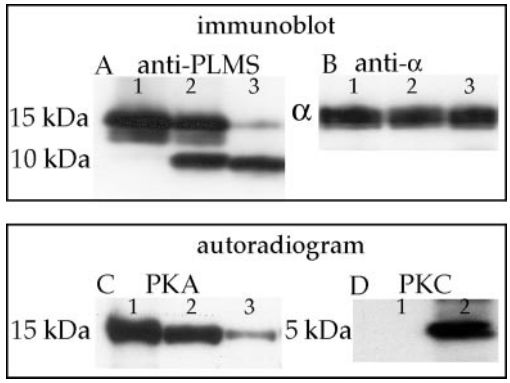

FIG. 7. **Tryptic cleavage of a 5-kDa peptide from PLMS and effects of PKA phosphorylation.** *A*, immunoblot of control and trypsin incubated samples. Trypsinization of the C terminus of PLMS was carried out on ice for 5 min in the presence of ~3 mg of purified protein, 1 mM of EDTA, 15% glycerol in the absence (*lane 1*), or presence (*lanes 2* and *3*) of 3 μg of trypsin. The proteolytic reactions contained concentrations of Na^+ and K^+ are as follows: *lane 1*, control (130 mM NaCl, no trypsin); *lane 2*, 130 mM Na^+; *lane 3*, 20 mM K^+. A PLMS-specific antibody that recognizes the N-terminal domain was used to probe the blot. Immunoblotting was as described under "Experimental Procedures." *B*, immunoblot of the α-subunit in the different trypsin-treated preparations was performed using an α-antibody as described under "Experimental Procedures." *C*, autoradiogram showing PKA phosphorylation of the different trypsin-treated shark membrane preparations in the presence of [^{32}P]ATP. It reveals the effect of PLMS truncation on PKA phosphorylation of the protein. There is a corresponding partial and complete loss of PLMS phosphorylation upon partial (in the presence of Na^+) and complete (in the presence of K^+) truncation of PLMS. *D*, autoradiogram showing PKC phosphorylation of the 5-kDa tryptic cleavage product of PLMS. Membranes were incubated in the absence (*lane 1*) or presence (*lane 2*) of trypsin. The C terminus of PLMS was separated from the membranes by centrifugation and concentrated using a Centricon tube with 10-kDa M_r cut-off. Subsequently, the supernatant containing the PLMS C terminus was phosphorylated by PKC and resolved by SDS-PAGE followed by autoradiography.

in SDS gels at a molecular mass of 15 kDa (Fig. 7*A*, *lane 1*), and it was intensively phosphorylated by PKA as indicated by the autoradiogram (Fig. 7*C*, *lane 1*). Incubation of the membranes on ice for 3–5 min at a trypsin to protein weight ratio of 0.001 in the presence of 130 mM Na^+ resulted in partial truncation of PLMS and the production of a new band on SDS-PAGE with an increased apparent mobility of about 10 kDa, (Fig. 7*A*, *lane 2*). In the presence of 20 mM K^+, the protein was highly sensitive to trypsin and virtually no intact PLMS could be detected (Fig. 7*A*, *lane 3*). Interestingly, increasing the ionic strength to 130 mM K^+ partially protected PLMS from proteolysis by trypsin (not shown), suggesting that the partial protection produced by the ion is not specific.

From the autoradiogram (Fig. 7*C*) it is indicated that the 5-kDa proteolytic fragment contained the phosphorylation motifs, because PKA phosphorylation of the 15-kDa PLMS decreased in parallel with the degree of cleavage (Fig. 7*C*, *lanes 2* and *3*). In addition, no phosphorylation was observed of products migrating with a mobility of 10 kDa in the gel. Therefore, truncation is associated with the concomitant loss of the ability of the resulting 10-kDa fragment of PLMS to become phosphorylated by PKA. The 5-kDa trypsin cleavage product was not observed in the SDS-gel, because it was removed by the washing and centrifugation performed after the trypsin treatment. However, autoradiography of a 5-kDa proteolytic fragment isolated and concentrated after the mild trypsin treatment demonstrated the phosphorylation of this fragment by PKC (Fig. 7*D*), indicating that it arises from PLMS and contained the PLMS multisite phosphorylation motif, because the phosphorylation of the α-subunit, the only other protein demonstrating significant phosphorylation, was unchanged (not shown). As seen from the immunoblot in Fig. 7*A* the 10-kDa proteolytic fragment can still be probed by the anti-PLMS antibody demonstrating that the epitope for binding the antibody is located upstream of the C-terminal phosphorylation domain.

The mild trypsinization conditions used to split PLMS had no direct effect on the α-subunit as confirmed by SDS-PAGE of the α-subunit in these preparations. As seen from the immunoblot in Fig. 7*B*, the α-subunit before and after trypsin treatment has the same mobility on SDS-PAGE, and probing of the α-subunit by anti-α-antibody showed no decrease in the intensity. Therefore, these conditions seem not to result in the well known proteolysis of the α-subunit N terminus in the presence of Na^+, nor was it sufficient for cleavage at the T1 position in the presence of K^+. This is to be expected, because controlled trypsinolysis of the α-subunit has previously been performed using a much higher trypsin to protein ratios and higher temperatures (49) than those used in the present experiments.

Functional Effects of C-terminal Cleavage of PLMS—To investigate any functional effects caused by the interaction between the C-terminal domain of PLMS and the Na,K-ATPase, we characterized the overall Na,K-ATPase catalytic reaction as well as some partial reactions in enzyme preparations where the 5-kDa phosphorylation domain of PLMS is either partially (130 mM Na^+) or completely (20 mM K^+) cleaved. The preparations were assayed using the following experimental approaches: (i) measurements of the Na^+-, K^+-, and ATP-activation of Na,K-ATPase catalytic activity at V_{max} conditions, (ii) activation of the Na-ATPase reaction by K^+ at low ATP concentration to measure the K^+ deocclusion pathway, (iii) measurements of the Na^+ activation curve at low ATP concentration to probe effects on the Na^+-binding affinity, (iv) measuring the vanadate sensitivity of control and PLMS-truncated preparations to probe the E_1/E_2 equilibrium, and (v) measurements of the low affinity ATP-supported transition $E_2(K) \rightarrow E_1(Na)ATP$ and the following phosphorylation reaction pathway leading to E_2-P using time resolved fluorescence measurements. The latter reactions include the major rate-limiting steps of the Na,K-ATPase catalytic cycle under physiological conditions (42, 50, 51).

Cation and ATP Substrate Dependence of Hydrolysis—Fig. 8 shows the Na^+ activation in the presence of 20 mM K^+ (*A*), the

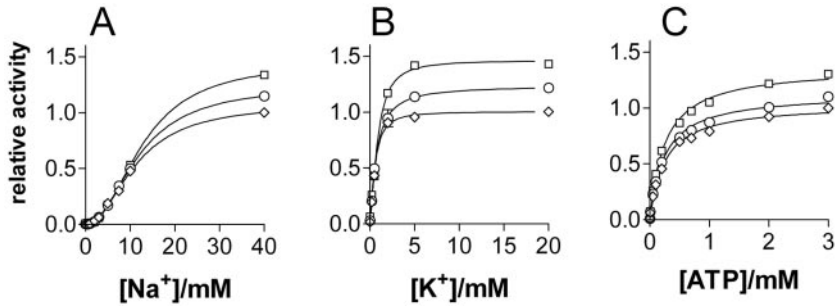

FIG. 8. **Ion- and substrate-dependent Na,K-ATPase activity in control membranes and in membranes where the C terminus of was PLMS truncated.** The hydrolytic activity of control (*Cont.*, ◇), partially truncated PLMS (*Tr-Na*$^+$, ○), and completely truncated PLMS (*Tr-K*$^+$, □) membrane preparations. *A*, Na^+-stimulated ATP hydrolysis in the presence of 3 mM ATP, 3 mM $MgCl_2$, and 20 mM KCl. Partial and complete truncation of PLMS resulted in about 25 and 50% stimulation of ATP hydrolysis, respectively ($p < 0.0001$). The apparent Na^+ affinities were: 11.2 ± 1.0, 12.1 ± 1.0, and 13.0 ± 1.0 mM, respectively. *B*, K^+-stimulated ATP hydrolysis in the presence of 3 mM ATP, 3 mM $MgCl_2$, and 130 mM NaCl. Partial and complete truncation of PLMS resulted in 30 and 60% stimulation of ATP hydrolysis, respectively ($p < 0.0001$). The apparent K^+ affinities were: 0.66 ± 0.08, 0.82 ± 0.006, and 0.99 ± 0.09 mM, respectively. *C*, ATP-stimulated Na,K-ATPase activity in the presence of 3 mM $MgCl_2$ 130 mM NaCl, and 20 mM KCl. Partial and complete truncation of PLMS resulted in about 15 and 40% stimulation of ATP hydrolysis, respectively ($p < 0.005$ and 0.0001, respectively). The apparent ATP affinities were: 0.247 ± 0.017, 0.246 ± 0.016, and 0.253 ± 0.014 mM, respectively. All reactions were performed in 30 mM histidine buffer, pH 7.00, and 2 μg of protein. P_i hydrolyzed from ATP was measured as described under "Experimental Procedures."

K^+ activation in the presence of 130 mM Na^+ (*B*), as well as the low affinity ATP activation (*C*) of the Na,K-ATPase in controls, partially truncated, and completely truncated PLMS preparations. Truncation, partial or complete, of PLMS leads to a significant increase in the hydrolytic activity of the Na,K-ATPase in all three cases. However, the apparent affinity for Na^+ in the presence of saturating K^+ (20 mM) did not change significantly, and this was also the case for the apparent K^+ affinity in the presence of saturating Na^+ (40 mM), and for the ATP affinity. The fact that V_{max} increases after PLMS truncation, however, indicates that some rate-determining steps of the Na,K-ATPase reaction must have been influenced.

Steady-state measurements of apparent ion and ATP affinities ($K_{0.5}$ or K_m) are not sensitive kinetic indications able to identify changes in single steps of the Na,K-ATPase reaction, because K_m contains all the rate constants around the Na,K-ATPase reaction cycle. A more precise indication of changes in the Na^+ binding affinity is provided by the ratio K_m/V_{max}, which will only contain rate constants of intermediates that are directly involved in the interaction with the ligand (52). Indeed, changes in the apparent affinity for cytoplasmic Na^+ (K'_{Na}) can be the result of a change in the Na^+ binding affinity or a change in the E_1/E_2 equilibrium. In the combined presence of Na^+ and K^+ changes in the competition between Na^+ and K^+ at the cytoplasmic face will also change the apparent Na^+ affinity. The latter was demonstrated to be the case for α1-HeLa cells transfected with γ_a or γ_b splice variants (11). If the Na^+ activation curve depicted in Fig. 8*A* is measured at different fixed K^+ concentrations, both V_{max} and K'_{Na} changes. A detailed kinetic analysis of cytoplasmic Na^+/K^+ competition of shark Na,K-ATPase has previously demonstrated that K^+_{cyt} inhibition of Na^+_{cyt} activation is a mixed multisite type inhibition in which K^+ competes with three similar site dissociation constants (53). In such models a linear relation between the calculated apparent Na^+ affinities and the K^+ concentration is expected, $K'_{Na} = K^o_{Na} + (K^o_{Na}/K_K)\cdot[K^+]$, as demonstrated by Garay and Garrahan (54). As seen from the results shown in Fig. 9*A* (note the $[K^+]$ is on a logarithmic scale) this linear relation apparently applies to the data giving a K^+ inhibition dissociation constant, K_K = 14 mM, and an apparent Na^+ affinity at zero $[K^+]$, K^o_{Na} = 4.4 mM. As indicated, no obvious change in the Na^+/K^+ competition is observed after PLMS truncation. Likewise, K^o_{Na} seems to change only slightly after PLMS truncation.

To investigate further if the Na^+ binding affinity changed after PLMS truncation, we measured the Na^+ activation in the absence of K^+ at low ATP concentration favoring formation of the E_1 conformation. Fig. 9*B* shows a typical experiment of the Na^+ activation of the enzyme in control and fully PLMS-truncated preparations. The apparent Na^+ affinity was 3.9 ± 1.0 mM for control and 2.9 ± 1.1 mM for PLMS-truncated samples ($p < 0.0001$). Thus, under these conditions the maximum activity increases and a small but significant increase in the apparent affinity for Na^+ are demonstrated, with a 1.6-fold increase in the K_m/V_{max} ratio after complete truncation of PLMS.

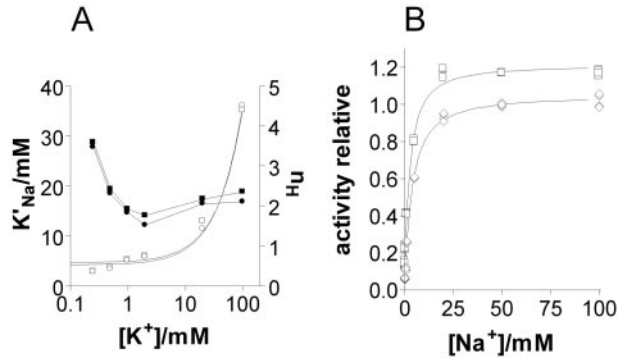

FIG. 9. **Effects of PLMS truncation on K^+/Na^+ antagonism and Na-ATPase activity of shark Na,K-ATPase.** *A*, the apparent affinity of Na^+ (K'_{Na}, *open symbols*) and the Hill coefficient (n_H, *closed symbols*) determined from Na^+ activation curves at different fixed K^+ concentrations as a function of the $[K^+]$ on a logarithmic scale. The relation between K'_{Na} and $[K^+]$ is given by the linear equation, $K'_{Na} = K^o_{Na} + (K^o_{Na}/K_K)\cdot[K^+]$ (given by the *curved lines* in the logarithmic scale) with a slope K^o_{Na}/K_K corresponding to 0.316 and intercept, K^o_{Na} = 4.35 mM, giving a K_K of 14 mM. The Hill coefficient decreased from about 3 to 2 as K^+ increased. *B*, the effects of PLMS truncation on Na-ATPase activity at low ATP. The Na-ATPase activity was measured in the presence of histidine 30 mM, pH 7.4, 1 mM $MgCl_2$, 1 μM Tris-ATP (containing 0.003 μCi of [^{32}P]ATP), and the sodium concentrations indicated, as described under "Experimental Procedures." Data are from double determination and expressed as a percentage of control in uncleaved Na,K-ATPase. The data were fitted with a sigmoid dose-response curve. The V_{max} under these conditions (measured at 100 mM NaCl) increased about 25% after truncation of PLMS ($p = 0.0001$). The $K_{0.5}$ is 3.94 ± 1.04 mM for control and 2.88 ± 1.05 mM for PLMS-truncated samples ($p < 0.0001$), whereas the Hill slope remained unchanged ($p = 0.7$). A representative of three independent experiments is shown.

K^+ Deocclusion—The K^+ activation of Na-ATPase activity at 1 μM ATP is a sensitive measure of the K^+ deocclusion pathway, $E_2(K) \rightarrow E_1$, as previously described (55). Fig. 10*A* shows

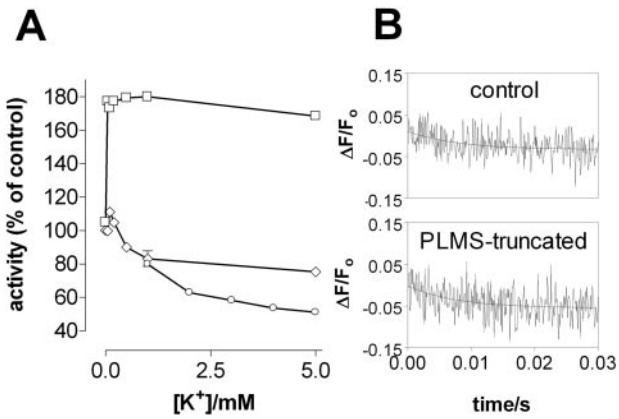

FIG. 10. **K^+ activation of Na-ATPase activity and the E_2(K) → E_1NaATP transition.** *A*, the ATP hydrolysis measured in the presence of 1 μM ATP (containing 0.2 pmol of [^{32}P]ATP), 15 mM NaCl, 2 mM $MgCl_2$, and varying K^+ concentrations as indicated in the figure, as described under "Experimental Procedures." ◇, control; □, PLMS cleaved preparation; and ○, N-terminal truncated Na,K-ATPase membrane preparations. Data are presented as percent of Na-ATPase activity measured in the absence of K^+. A representative of three independent experiments is shown. Values are means ± S.E. *B*, the rapid mixing stopped-flow RH421 fluorescence response of control membranes and membranes with the C terminus of PLMS fully truncated. One syringe contained 30 mM histidine buffer, pH 7.5, 1.0 mM KCl, 20 μg of protein, 0.5 mM CDTA, 0.1 mM EGTA, and 0.4 μg of RH421. The second syringe contained the same buffer plus 100 mM NaCl, 2.0 mM KCl, 2.0 mM TrisATP, 0.5 mM CDTA, and 0.1 mM EGTA. The pH value was adjusted to 7.5 using *N*-methyl-D-glucamine. The data were fitted with a mono-exponential time function with rate constants: control, 125 ± 16.2 s^{-1}; PLMS-truncated enzyme, 106 ± 10.3 s^{-1}. The rate constant for PLMS-truncated enzyme differs insignificantly from control enzyme.

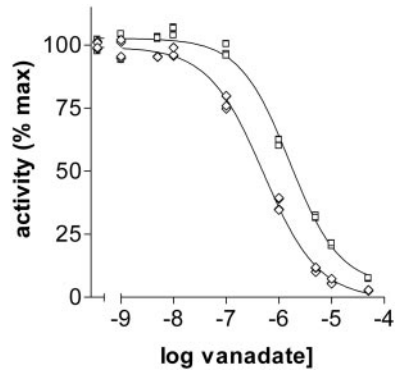

FIG. 11. **Vanadate sensitivity of shark Na,K-ATPase membrane preparations.** ATP hydrolysis was measured in the presence of 1.5 mM Tris-ATP, 100 mM NaCl, 20 mM KCl, 2 mM $MgCl_2$, and vanadate concentrations as denoted in the figure. Data are from double determination and expressed as percentage of control measured in the absence of vanadate. The data were fitted with a sigmoid dose-response curve. The $K_{0.5}$ is 0.505 ± 0.001 μM for control and 1.600 ± 0.001 μM for the PLMS-truncated sample (significantly different, $p < 0.0001$). A representative of two independent measurements is shown.

experiments where the K^+ sensitivity of Na-ATPase at 1 μM ATP, which is only sufficient to saturate the high affinity ATP binding site, is measured. Addition of only 15 mM Na^+ ensures that the enzyme conformation is not permanently locked in the E_1 conformation. Without K^+ only Na-ATPase activity is measured, in which the deocclusion reaction (of Na^+) is not rate limiting at low ATP concentrations (56). Addition of K^+ to the medium at conditions where only the high affinity ATP site is occupied will induce dephosphorylation of the enzyme and production of the E_2(K) form. Without low affinity ATP-binding K^+ deocclusion is rate limiting, and the hydrolytic activity can be inhibited (57). Fig. 10*A* shows that this is actually the case for the control enzyme. However, after truncation of PLMS, the hydrolytic activity is stimulated about 200% by the addition of low K^+ concentrations, indicating that some of the steps in the K^+ deocclusion pathway are accelerated, either the spontaneous and/or the ATP-supported K^+ deocclusion, because truncation of PLMS had no effect on the ATP affinity at the low affinity site (see Fig. 8*C*).

That the former could be the case was indicated by measurements of the main rate-limiting E_2(K) → E_1NaATP reaction at physiological conditions, including the low affinity ATP binding (42, 50, 51). This reaction can be measured by stopped-flow fluorescence using the potential sensitive styryl dye RH421 (42). Initially, the enzyme is incubated in an E_2-supporting buffer like histidine in the absence of Na^+ and with CDTA to bind any residual Mg^{2+}. The enzyme is then rapidly mixed with Na^+ and ATP to induce the transition to E_1NaATP, whereas the following phosphorylation step is prevented by the absence of Mg^{2+}. The transition from E_2 to E_1 is followed by a small drop in fluorescence ($\Delta F/F_o \sim 5\%$), which can be measured, as demonstrated in Fig 10*B*. As seen from the figure, PLMS-truncated preparations and controls gave identical fluorescence decays indicating no significant effects on this reaction.

The E_1/E_2 Equilibrium—Subsequently, the effect of PLMS cleavage on the vanadate sensitivity of Na,K-ATPase was studied. Orthovanadate is a transition state analogue of inorganic phosphate that binds preferentially to the E_2 conformation of P-type ATPases. Thus, the sensitivity of Na,K-ATPase to inhibition by vanadate reflects the proportion of the enzyme adopting an E_2 conformation. As can be seen from Fig. 11 truncation of PLMS produced an enzyme preparation more resistant to vanadate ($K_I \sim 1.60 \pm 0.001$ μM) when compared with control ($K_I \sim 0.50 \pm 0.001$ μM, $p < 0.0001$), suggesting that PLMS truncation stabilized the E_1 conformation of the enzyme. The vanadate sensitivity of the shark enzyme is comparable to the mammalian kidney α1 enzyme (56, 57).

The Phosphorylation/Dephosphorylation Reactions—The phosphorylation reaction was investigated by stopped-flow measurements using the membrane probe RH421 (41, 58). This styryl dye partitions into the membrane containing Na,K-ATPase and is sensitive to the formation of E_2-P.

The phosphorylation reactions in Fig. 12*A* show the formation of E_2-P from mixing of the enzyme in the presence of 30 mM Na^+ with 3 mM MgATP and thus represents the reactions E_1Na → E_1NaATP → $E_1 \sim P \rightarrow E_2$-P. In shark Na,K-ATPase the initial phosphoryl transfer and formation of E_1~P are faster than the formation of E_2-P, at least at temperatures below 15 °C (58). Thus, the stopped-flow fluorescence reaction mainly measures the rate of the $E_1 \sim P \rightarrow E_2$-P reaction. As seen from Fig. 12*A* this rate increases after PLMS truncation, from about 60 to 80 s^{-1} ($p = 0.009$).

The dephosphorylation reaction was measured using enzyme pre-treated with ATP in the presence of Na^+ and Mg^{2+} to induce a maximum steady-state level of the E_2P form, as described above for the phosphorylation reaction. The enzyme is then reacted with K^+ in a rapid-mixing stopped-flow experiment using RH421 to detect the decrease of fluorescence as the E_2P phosphoenzyme is hydrolyzed. As seen from Fig. 12*B*, the rate of the K^+-activated dephosphorylation is not significantly different from the control enzyme and PLMS-truncated enzyme.

DISCUSSION

PLMS Sequence—The nucleic acid sequence encoded a 94-amino acid coding sequence of PLMS (Fig. 1), which was identical at the N terminus to the partial sequence previously determined by protein sequencing of the purified protein (21), with the exception that leucine replaced lysine at positions 19

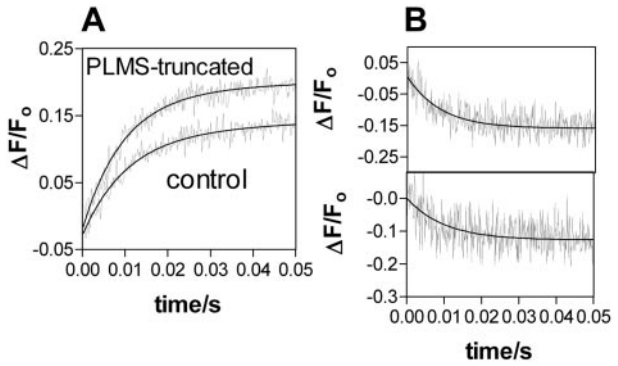

FIG. 12. **Rapid mixing stopped-flow fluorescence following ATP phosphorylation and K^+-supported dephosphorylation.** *A*, rapid mixing stopped-flow RH421 fluorescence response to phosphorylation by ATP at 20 °C of control membranes and membranes with the C terminus of PLMS fully truncated. One syringe contained 10 mM Hepes buffer, 10 mM MES buffer, 16 mM NaCl, 20 μg of protein, and 0.4 μg of RH421. The second syringe contained 10 mM HEPES/MES buffer plus 2 mM ATP, and 4 mM $MgCl_2$. The pH value was adjusted to 7.5 using *N*-methyl-D-glucamine. The results from controls have been downward-shifted to separate it from the results from the PLMS-truncated enzyme. Fitting of monoexponentials to the data gave the following rate constant values: control enzyme, 60.5 ± 1.3 s^{-1}; truncated enzyme, 80.2 ± 1.8 s^{-1}. The rate constant for PLMS-truncated enzyme is significantly larger than that for control enzyme ($p = 0.009$). *B*, rapid mixing stopped-flow RH421 fluorescence response of ATP-phosphorylated enzyme to K^+. The enzyme (~20 μg) was first phosphorylated in syringe 1 in the presence of 10 mM NaCl, 2 mM TrisATP, 10 mM Hepes/Mes buffer, pH 7.5, 4 mM $MgCl_2$, and 0.4 μg of RH421. The enzyme was then rapidly mixed with 10 mM KCl in the same HEPES/MES buffer. The monoexponential fluorescence decayed with rate constants: control, 109 ± 3.9 s^{-1}; PLMS-truncated enzyme, 93.3 ± 4.9 s^{-1}. The rate constant for PLMS-truncated enzyme differed insignificantly from control enzyme.

and 24. The reason for this difference in sequence is unknown but may relate to errors in reading the protein sequence as sequencing progresses to the C-terminal end of the peptide. Alternatively, it is possible that the cloned cDNA is a closely related isoform of the gel-extracted protein. Further molecular studies will be required to examine the possibility of other PLMS isoforms. *Squalus* PLMS exhibits highest homology to MAT-8 or F*X*YD3 (39–45% amino acid identity and 59–67% amino acid similarity). Because the amino acid sequence homology between the zebrafish F*X*YD9(dr) and the human F*X*YD6 genes (43% identity and 64% similarity) is not considered close enough for these two proteins to be identified as orthologues, we suggest that, until more information is available regarding the evolution of the F*X*YD family genes, the PLMS gene should be designated as F*X*YD10(sa).

Although the amplified and cloned cDNA, which contains the entire coding sequence of PLMS, was only 445 bp long, Northern blot analyses revealed the presence of a major 3.8-kb transcript. In all tissues that expressed this 3.8-kb mRNA, additional minor transcripts of 0.8, 1.1, 1.3, and 2 kb were also detected, which were most apparent in the rectal gland that exhibited the highest overall levels of expression. Further 3′- and 5′-RACE amplifications using a range of annealing temperatures (52–62 °C) with extension times up to 4 min failed to reveal any larger amplicons. Although there is no experimental evidence explaining these observations, it is possible that the Marathon oligo(dT) cDNA synthesis primer has misprimed on the PLMS mRNA at a short poly(A) tract some 100 bp to the 3′ of the coding sequence (Fig. 1).

The first 20 amino acid residues are assumed to form a cleavable signal sequence as found for other F*X*YD proteins except the γ and F*X*YD7 resulting in a mature protein containing 74 amino acid residues with a calculated molecular mass of 8216 Da. Thus, the electrophoretic mobility (15 kDa) of this small protein differs significantly from the protein mass as for the other hydrophobic F*X*YD proteins. The previous finding that PLMS is resolved as a doublet on two-dimensional SDS-PAGE (21) could suggest that PLMS may also undergo co- or post-translational processing, as is the case for the γ (12, 59) and possibly also for CHIF (23) and F*X*YD7 (24).

As noted in the sequence the serine immediately adjacent to the plasma membrane on the cytoplasmic side, which is conserved in all known mammalian F*X*YD sequences, is changed to an alanine in PLMS. This serine is located inside a conventional PKC phosphorylation motif, and in γ it can be phosphorylated by PKC *in vitro* in the presence of detergent (60).

Cell and Tissue Distribution—The co-location of PLMS with Na,K-ATPase on basolateral membranes of rectal gland cells (Figs. 5 (*A* and *C*) and 6 (*A* and *B*)) fits the physiological role of this F*X*YD protein as a specific regulator of Na,K-ATPase. The shark rectal gland is the organ responsible for the extra-renal salt secretion and has served as an epithelial transport model for secretory epithelial organs where chloride secretion relies on the coordination and polarized localization of at least five transport pathways: Cl^- is initially concentrated inside the cell by the basolateral Na-K-2Cl co-transporter and diffuses to the lumen across the apical membrane via the chloride channels (cystic fibrosis transmembrane conductance regulator). The K^+ ions are re-circulated by basolateral K^+ channels and the energy for the Cl^- uptake is provided by the Na,K-ATPase that is also located on basolateral membranes (61). The transcellular Cl^- transport is accompanied by a paracellular Na^+ transport across the tight junctions (Fig. 5, *A–C*). In accordance with this model, the present results have indicated co-localization of Na,K-ATPase and PLMS on basolateral membranes in the rectal gland cells. By the recognition of the new functional role of F*X*YD proteins in regulation of the Na,K-ATPase the transport pathways responsible for Cl^- secretion seem all to be controlled by protein kinase/phosphatase regulation (62–64).

Functional Effects—In the present study we demonstrate that in Na,K-ATPase membrane preparations the C-terminal protein kinase phosphorylation domain of PLMS can be cleaved by controlled trypsin treatment. Specific PLMS cleavage without cleavage of the N-terminal Na,K-ATPase α-subunit can be obtained at low trypsin to Na,K-ATPase ratio, low temperature, short incubation time, and 20 mM K^+ (Fig. 7). It is well known that, in the presence of K^+, trypsin treatment leads to cleavage of the mammalian α-subunit near the middle but does not cleave off the small N terminus (49). Nevertheless, the possibility that the N terminus of the Na,K-ATPase α-subunit may itself be cleaved by the trypsin treatment used to cleave PLMS was excluded by several controls. On the one hand, cleavage of the N terminus of the Na,K-ATPase α-subunit decreases the hydrolytic activity significantly (49, 65), whereas the mild trypsin treatment used to specifically cleave PLMS leads to a significant increase in maximum hydrolytic activity (Fig. 8). Furthermore, after PLMS truncation the α-subunit is still phosphorylated by PKC at the N-terminal site (data not shown). Finally, at conditions used for PLMS cleavage the well known increase in mobility of the N-terminal truncated α-subunit on SDS-PAGE is absent (Fig. 7*B*). It is interesting to note, however, that the opposite is not true, *i.e.* at conditions where the N-terminal domain of the α-subunit is cleaved by trypsin, the C terminus of PLMS also becomes cleaved. In contrast, controlled N-terminal truncation of kidney Na,K-ATPase α-subunit leaves the γ intact (not shown).

Specific cleavage of the C terminus of PLMS activates the Na,K-ATPase at V_{max} conditions indicating effects on rate-determining steps. At saturating substrate concentrations the rate-limiting steps are the $E_2 \rightarrow E_1$ transition associated with

low affinity ATP-supported K^+ deocclusion and binding of cytoplasmic Na^+ (51) and the $E_1 \sim P \rightarrow E_2$-P transition, at least at temperatures below 15 °C (58). Indeed, detailed investigations of the partial reactions showed that some steps along the K^+ deocclusion pathway $E_2(K_2) \rightarrow E_1$ are accelerated after PLMS truncation (Fig. 10*A*) and shifted the E_1/E_2 conformational equilibrium toward the E_1 form, as shown by the lower vanadate sensitivity (Fig. 11). These effects may contribute to the small increase in apparent Na^+ affinity (Fig. 9*B*). The deocclusion supported by low affinity ATP binding (Fig. 10*B*), as well as the apparent ATP affinity (Fig 8*C*) was unchanged. PLMS-truncation did not change the K^+-supported dephosphorylation, whereas the ATP-phosphorylation reaction measured by the increase in RH421 fluorescence was increased, indicating that the partially rate-limiting reaction $E_1 \sim P \rightarrow E_2$-P is accelerated. Thus, the increased V_{max} induced by specific PLMS truncation is probably an effect mainly on the catalytic site phosphorylation reaction and not on the main rate-limiting step, the K^+ deocclusion supported by low affinity ATP binding.

A major effect of F*X*YD proteins hitherto investigated relates to modulation of apparent Na^+ or K^+ affinities (19, 20). A similar situation seems to exist for the PLMS/Na,K-ATPase system where PLMS truncation increases the apparent cytoplasmic Na^+ affinity (Fig. 9*B*) without affecting the Na^+/K^+ competition at the cytoplasmic sites (Fig. 9*A*). Thus PLMS association decreases the Na^+ affinity. This is in agreement with recent studies on mammalian PLM where co-expression of the α-subunit and PLM in *Xenopus* oocytes resulted in a decrease in the apparent cytoplasmic Na^+ affinity of Na,K-ATPase (22). Thus, association of F*X*YD1 proteins with the Na,K-ATPase leads in both cases to a decreased Na^+ affinity and inhibition of enzyme activity, whereas dissociation of the F*X*YD1 proteins results in stimulation of hydrolytic activity. Other F*X*YD proteins have different patterns of effects: association of γ (F*X*YD2) with Na,K-ATPase has been shown to increase the apparent ATP affinity by supporting the E_1 conformation of the enzyme and to decrease the apparent affinity for cytoplasmic Na^+, which apparently is an effect secondary to an increased antagonism of cytoplasmic K^+ to activation by Na^+ (10, 11). In other investigations the change in apparent affinity for Na^+ could not be unambiguously assigned to such increased Na^+/K^+ competition alone but also indicated γ induced changes in the intrinsic binding affinity for Na^+ (59). Effects on the extracellular K^+ affinity of both splice variants of γ have also been reported (11, 59). Co-expression of the F*X*YD4 protein CHIF with rat α1 increased the apparent affinity for cytoplasmic Na^+, without affecting the K^+ affinity or V_{max} (23, 66). It should be noted, however, that assignment of changes in apparent ion affinities from steady-state measurements to specific steps in the reaction mechanism might be difficult. In co-expression experiments where changes in V_{max} are not usually controlled, this can be important, because variations in V_{max} in itself are expected to change the apparent ion affinities in a ping-pong kinetic model (67).

It is interesting to note that the functional effects following cleavage of the C-terminal domain of PLMS resemble in some aspects the effects reported after truncation of the N-terminal domain of the rat kidney α-subunit. Thus, in mutagenesis studies deletion of up to 40 N-terminal residues of the α-subunit accelerates K^+ deocclusion at limited ATP concentrations and shifts the E_1/E_2 conformation of the enzyme toward the E_1 form, whereas further N-terminal deletions reversed this effect (57). From these experiments it was suggested that the N-terminal domain of the α-subunit play an autoregulatory role in controlling the E_1/E_2 conformation of the enzyme by interaction of the N terminus/M2-M3 loop with the large catalytic domain. It is possible, therefore, that other regulatory mechanisms may act by controlling interdomain interaction thereby affecting the E_1/E_2 conformational transition of the enzyme.

Although the domains within PLMS that are important for the regulatory interaction with the Na,K-ATPase α-subunit have not yet been directly identified, indirect evidence indicates that sites in both the cytoplasmic and membrane regions of PLMS may be important. Thus, sub-critical micelle concentrations of detergent that impair the protein-protein hydrophobic interactions relieved PLMS inhibition of Na,K-ATPase (21). Previous investigations have suggested γ to be localized close to the C terminus of the α-subunit (27, 28). Compared with the three-dimensional structure determination of SERCA (68), this position would also be close to the N terminus/M1-M2 transmembrane segments of the Na,K-ATPase α-subunit, *i.e.* within the same area suggested to be important for autoregulation (57). Furthermore cytoplasmic sites of PLMS near to the C-terminal protein kinase phosphorylation motif must be important for the PLMS inhibition of Na,K-ATPase, which can be relieved by PKC phosphorylation of PLMS (21). We suggest that this interaction is between sites in the C-terminal part of PLMS and the A domain of the α-subunit and that inhibition is due to restriction of the A domain movement (20). This is supported by the specific effects of PLMS cleavage on the $E_1 \sim P \rightarrow E_2$-P reaction and on the subsequent K^+ deocclusion reactions demonstrated in the present investigation. Such an explanation is also in accordance with a recent study using SERCA treated with proteinase K that cleaves a loop linking the A domain with M3 (69). In such preparations the formation of E_2P from E_1P is strongly reduced indicating that the flexibility of the A domain is important for this conformational transition.

In summary, the data presented in this study suggest an important role for PLMS in the regulation of Na,K-ATPase activity in shark rectal glands. The induced dissociation of PLMS from the Na,K-ATPase by proteolytic cleavage of the C-terminal multisite phosphorylation domain resulted in an increase in the rates of both the phosphorylation at the catalytic site and the subsequent K^+ deocclusion. The sequence of PLMS and its localization in the shark rectal gland cells should represent a firm starting point for further studies aiming at identifying the physiological role of PLMS in the hormonal control of Na,K-ATPase activity in this model transport epithelium and to characterize the molecular interaction of the two proteins responsible for this regulation.

Acknowledgment—We thank Niels Rüdiger for his help in designing the primers to PLMS during the early stages of the cloning work.

REFERENCES

1. Kaplan, J. H. (2002) *Annu. Rev. Biochem.* **71,** 511–535
2. Cornelius, F., Mahmmoud, Y. A., and Christensen, H. R. Z. (2001) *J. Bioenerg. Biomemb.* **33,** 415–423
3. Kimura, Y., Kurzydlowski, K., Tada, M., and MacLennan, D. H. (1997) *J. Biol. Chem.* **272,** 15061–15064
4. Kimura, Y., Asahi, M., Kurzydlowski, K., Tada, M., and MacLennan, D. H. (1998) *J. Biol. Chem.* **273,** 14238–14241
5. Reddy, L. G., Autry, J. M., Jones, L. R., and Thomas, D. D. (1999) *J. Biol. Chem.* **274,** 7649–7655
6. Odermat, A., Becker, S., Khanna, V. K., Kurzydlowski, K., Leisner, E., Pette, D., and MacLennan, D. H. (1998) *J. Biol. Chem.* **273,** 12360–12369
7. Russell Tupling, A., Asahi, M., and MacLennan, D. H. (2002) *J. Biol. Chem.* **277,** 44740–44746
8. Béguin, P., Wang, X., Firsov, D., Puoti, A., Claeys, D., Horisberger, J.-D., and Gerring, K. (1997) *EMBO J.* **16,** 4250–4260
9. Therien, A. G., Goldshleger, R., Karlish, S. J. D., and Blostein, R. (1997) *J. Biol. Chem.* **272,** 32628–32634
10. Therien, A. G., Karlish, S. J. D., and Blostein, R. (1999) *J. Biol. Chem.* **274,** 12252–12256
11. Pu, H. X., Cluzeaud, F., Goldshleger, R., Karlish, S. J. D., Farman, N., and Blostein, R. (2001) *J. Biol. Chem.* **276,** 20370–20378
12. Arystarkhova, E., Wetzel, R. K., Asinovski, N. K., and Sweadner, K. J. (1999) *J. Biol. Chem.* **274,** 33183–33185

13. Sweadner, K. J., and Rael, E. (2000) *Genomics* **68,** 41–56
14. Palmer, C. J., Scott, D., and Jones, L. R. (1991) *J. Biol. Chem.* **266,** 11126–11130
15. Minor, N. T., Sha, Q., Nichols, C. G., and Mercer, R. W. (1998) *Proc. Natl. Acad. Sci. U. S. A.* **95,** 6521–6525
16. Morrison, B. W., Moorman, J. R., Kowdley, G. C., Kobayashi, Y. M., Jones, L. R., and Leder, P. (1995) *J. Biol. Chem.* **270,** 2176–2182
17. Attali, B., Latter, H., Rachamim, N., and Garty, H. (1995) *Proc. Natl. Acad. Sci. U. S. A.* **92,** 6092–6096
18. Fu, X., and Kamps, M. P. (1997) *Mol. Cell. Biol.* **17,** 1503–1512
19. Crambert, G., and Geering, K. (2003) *Science's STKE* http://stke.sciencemag.org/cgi/content/full/sigtrans;2003/166/re1
20. Cornelius, F., and Mahmmoud, Y. A. (2003) *News. Physiol. Sci.* **18,** 119–124
21. Mahmmoud, Y. A., Vorum, H., and Cornelius, F. (2000) *J. Biol. Chem.* **274,** 35969–35977
22. Crambert, G., Fuzesi, M., Garty, H., Karlish, S., and Geering, K. (2002) *Proc. Natl. Acad. Sci. U. S. A.* **99,** 11476–11481
23. Béguin, P., Crambert, G., Guennoun, S., Garty, H., Horisberger, J. D., and Gerring, K. (2001) *EMBO J.* **20,** 3993–4002
24. Béguin, P., Crambert, G., Monnet-Tschudi, F., Uldry, M., Horisberger, J. D., Garty, H., and Geering, K. (2002) *EMBO J.* **21,** 3264–3273
25. Meij, I. C., Koenderink, J. B., van Bokhoven, H., Assink, K. F., Groenestege, W. T., de Pont, J. J., Bindels, R. J., Monnens, L. A., van den Heuvel, L. P., and Knoers, N. V. (2000) *Nat. Genet.* **26,** 265–266
26. Aizman, R., Asher, C., Fuzesi, M., Latter, H., Lonai, P., Karlish, S. J. D., and Garty, H. (2002) *Am. J. Physiol.* **283,** F569–F577
27. Hebert, H., Purhonen, P., Vorum, H., Thomsen, K., and Maunsbach, A. V. (2001) *J. Mol. Biol.* **314,** 479–494
28. Donnet, C., Arystarkhova, E., and Sweadner, K. J. (2001) *J. Biol. Chem.* **276,** 7357–7365
29. Pu, X. P., Scanzano, R., and Blostein, R. (2002) *J. Biol. Chem.* **277,** 20270–20276
30. Lindzen, M., Aizman, R., Lifshitz, Y., Lubarski, I., Karlish, S. J., and Garty, H. (2003) *J. Biol. Chem.* **278,** 18738–18743
31. Cornelius, F., and Mahmmoud, Y. A. (2003) *Ann. N. Y. Acad. Sci. U. S. A.* **986,** 579–586
32. Chomczynski, P., and Sacchi, N. (1987) *Anal. Biochem.* **162,** 156–159
33. Cutler, C. P., Brezillon, S., Bekir, S., Sanders, I. L., Hazon, N., and Cramb, G. (2000) *Am. J. Physiol.* **279,** R222–R229
34. Sambrook, J., and Gething, M. J. (1989) *Nature* **342,** 224–225
35. Manusbach, A. B. (1998) in *Cell Biology: A Laboratory Handbook*, Vol. 3, 2nd Ed. (Celis, J. E., ed) pp. 268–275, Academic Press, San Diego
36. Skou, J. C., and Esmann, M. (1979) *Biochim. Biophys. Acta* **567,** 436–444
37. Peterson, G. L. (1977) *Anal. Biochem.* **83,** 346–356
38. Lindberg, O., and Ernster, L. (1956) *Methods Biochem. Anal.* **3,** 1–12
39. Laemmli, U. K. (1970) *Nature* **227,** 680–685
40. Møller, J. V., Ning, G., Maunsbach, A. B., Fujimoto, K., Asai, K., Juul, B, Lee, Y.-J., de Garcia, A. G., Falson, P., and le Maire, M. (1997) *J. Biol. Chem.* **272,** 29015–29032
41. Fedosova, N. U., Cornelius, F., and Klodos, I. (1995) *Biochemistry* **34,** 16806–16814
42. Humphrey, P. A., Lupfert, C., Apell, H. J., Cornelius, F., and Clarke, R. J. (2002) *Biochemistry* **41,** 9496–9507
43. Chen, L.-S. K., Lo, C. F., Numann, R., and Cuddy, M. (1997) *Genomics* **41,** 435–443
44. Nielsen, H., Engelbrecht, J., Brunak, S., and van Heine, G. (1997) *Prot. Eng.* **10,** 1–6
45. Bulger, R. E. (1963) *Anat. Rec.* **147,** 95–127
46. Goertmiller, C. C., Jr., and Ellis, R. A. (1976) *Cell Tissue Res.* **175,** 101–112
47. Eveloff, J., Karnaky, K. J., Jr., Silva, P., Epstein, F. H., and Kinter, W. B. (1979) *J. Cell Biol.* **83,** 16–32
48. Maunsbach, A. B., and Boulpaep, E. L. (1984) *Am. J. Physiol.* **246,** F710–F724
49. Jørgensen, P. L., and Farley, R. A. (1988) *Methods Enzymol.* **156,** 291–303
50. Karlish, S. J. D., and Yates, D. (1978) *Biochim. Biophys. Acta* **527,** 115–130
51. Lupfert, C., Grell, E., Pintschovius, V., Apell, H. J., Cornelius, F., and Clarke, R. J. (2001) *Biophys J.* **81,** 2069–2081
52. Plesner, I. W. (1986) *Biochem. J.* **239,** 175–178
53. Cornelius, F. (1992) *Biochim. Biophys. Acta* **1108,** 190–200
54. Garay, R. P., and Garrahan, P. J. (1973) *J. Physiol.* **231,** 297–325
55. Daly, S. E., Lane, L. K., and Blostein, R. (1996) *J. Biol. Chem.* **271,** 23683–23689
56. Cornelius, F., and Skou, J. C. (1991) *Biochim. Biophys. Acta* **1067,** 227–234
57. Segall, L., Lane, L. K., and Blostein, R. (2002) *J. Biol. Chem.* **277,** 35202–35209
58. Cornelius, F. (1999) *Biophys. J.* **77,** 934–942
59. Arystarkhova, E., Donnet, C., Asinovski, N. K., and Sweadner, K. J. (2002) *J. Biol. Chem.* **277,** 10162–10172
60. Mahmmoud, Y. A., and Cornelius, F. (2002) *Biophys. J.* **82,** 1909–1917
61. Silva, P., Solomon, R. J., and Epstein, F. H. (1996) *Kindey Int.* **49,** 1552–1556
62. Bear, C. E., Li, C. H., Kartner, N., Bridges, R. J., Jensen, T. J., Ramjeesingh, M., and Riordan, J. R. (1992) *Cell* **68,** 809–818
63. Xu, Z. C., Yang, Y., and Hebert, S. C. (1996) *J. Biol. Chem.* **271,** 9313–9319
64. Darman, R. B., Flemmer, A., and Forbush, B. (2001) *J. Biol. Chem.* **276,** 34359–34362
65. Krüger, A. K., Mahmmoud, Y. A., and Cornelius, F. (2003) *Ann. N. Y. Acad. Sci. U. S. A.* **986,** 541–542
66. Garty, H., Lindzen, M., Scanzano, R., Aizman, R., Fuzesi, M., Goldshleger, R., Farman, N., Blostein, R., and Karlish, S. J. D. (2002) *Am. J. Physiol.* **283,** F607–F615
67. Cleland, W. W. (1963) *Biochim. Biophys. Acta* **944,** 188–196
68. Toyoshima, C., Nakasako, M., Nomura, H., and Ogawa, H. (2000) *Nature* **405,** 647–655
69. Møller, J. V., Lenoir, G., Marchand, C., Montigny, C., le Maire, M., Toyoshima, C., Juul, B. S., and Champeil, P. (2002) *J. Biol. Chem.* **277,** 38647–38659

Regulation of Na,K-ATPase by PLMS, the Phospholemman-like Protein from Shark: MOLECULAR CLONING, SEQUENCE, EXPRESSION, CELLULAR DISTRIBUTION, AND FUNCTIONAL EFFECTS OF PLMS

Yasser A. Mahmmoud, Gordon Cramb, Arvid B Maunsbach, Christopher P. Cutler, Lara Meischke and Flemming Cornelius

J. Biol. Chem. 2003, 278:37427-37438.
doi: 10.1074/jbc.M305126200 originally published online July 21, 2003
